J. Fluid Mech. (1969), *vol.* 38, *part* 1, *pp.* 109–125
Printed in Great Britain

The interaction region in the boundary layer of a shock tube

By S. D. BAN
Fluid and Gas Dynamics Division, Battelle Memorial Institute, Columbus, Ohio
AND G. KUERTI†
Case Western Reserve University, Cleveland, Ohio

(Received 10 August 1968 and in revised form 22 January 1969)

Velocity and temperature boundary layers developed on a plane wall by ideal shock-tube flow are considered for weak shock and expansion waves. Analytically, the boundary layer consists of three regions, bounded by (1) expansion-wave head, (2) diaphragm location, (3) contact discontinuity, (4) shock. The flow fields (1, 2) and (3, 4) are, essentially, known. In the interaction region (2, 3), these flow fields merge, the governing equations are 'singular parabolic' and admit boundary conditions usually associated with elliptic equations. It is convenient to replace the weak expansion wave in the main flow by a line discontinuity. A consistent linearization scheme can now be devised to obtain the solution in the three regions. In (2, 3), the resulting linear singular parabolic equations for the first-order solutions are solved successfully by an iterative finite difference method, normally applied to elliptic equations.

1. Introduction

The unsteady one-dimensional flow pattern that develops in the ideal shock tube has been known in its essentials since Riemann's famous paper in 1860. This flow develops, after the diaphragm initially separating high ($x < 0$) and low pressure ($x > 0$) motionless gases in the tube has been removed at $t = 0$. The well-known (x, t)-diagram of the motion is shown in figure 1 with the initial diaphragm position at the origin of the (x, t)-plane. The resulting boundary layer at $t = t^*$ is also sketched.

Here we consider the velocity and enthalpy boundary layers developed on a plane wall by the ideal outer flow pattern. However, we treat only weak waves so that the expansion region EW can be approximated by a line discontinuity across which the isentropic expansion-fan relations hold. This situation is shown in figure 2.

Several authors have considered the boundary layer developed by parts of the shock-tube flow. Mirels (1955) examined the boundary layer behind a shock advancing along a plane wall into a stationary fluid. His solution is limited to the part of the boundary layer beneath the region M in figures 1 and 2. Cohen (1957)

† At present at the University of Rostock, G.D.R.

considered the boundary layer developed by a centerd expansion fan advancing into a stationary fluid which is exactly the case in region EW of figure 1. Mirels (1956) extended his previous work to boundary layers behind infinitely thin

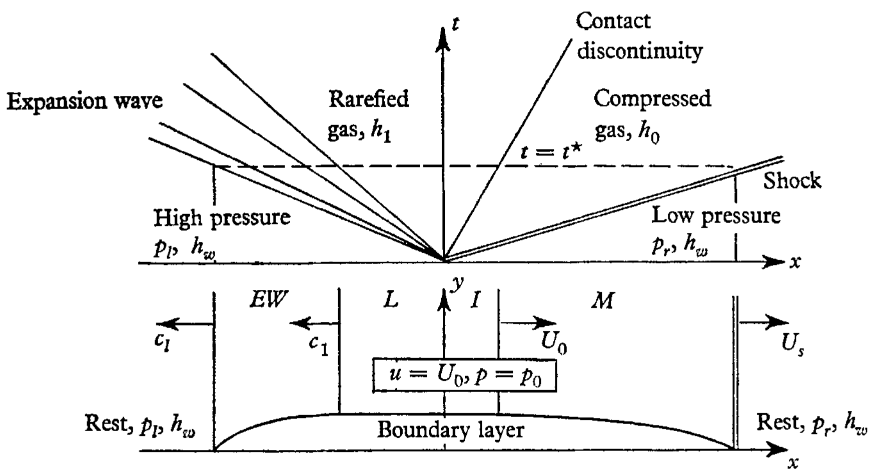

FIGURE 1. Ideal shock-tube flow.

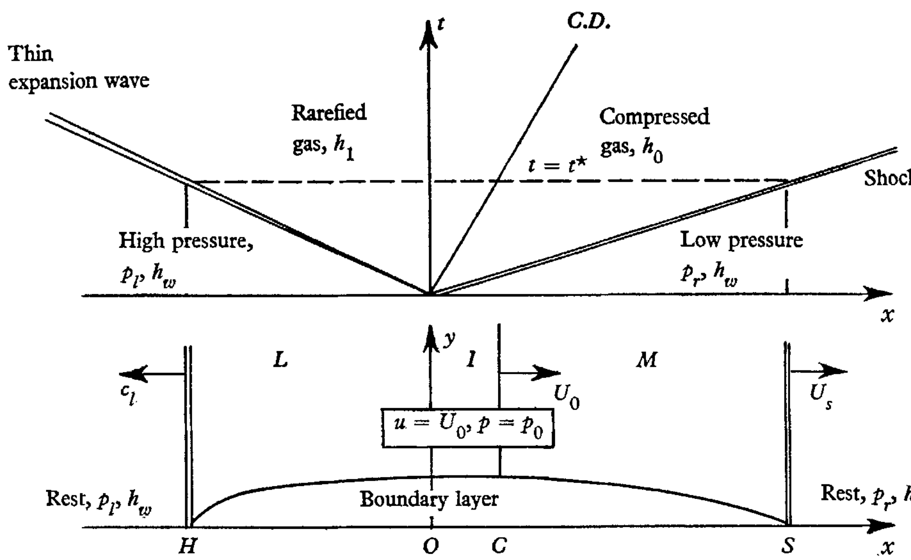

FIGURE 2. Weak wave shock-tube flow.

expansion waves as is the case of region L of figure 2. Becker (1962) attempted to extend the validity of Cohen's (1957) solution to the L–I boundary by a continuation procedure.

Thus, the boundary layer beneath region M has been well discussed, those beneath regions EW and L have been approximately treated while the mathematically more difficult region I has been neglected entirely. It is for this reason that in the present work we concentrate wholely on the I region (I denotes 'interaction' between the L and M regions as in Lam & Crocco (1958)), and approximate the EW region as in figure 2.

Two papers are of interest for the boundary-layer study in the I region. Stewartson (1951) studied the fluid motion induced by the uniform motion of a semi-infinite plate in its own plane ($x > 0$). The plate velocity U_∞ is acquired suddenly at $t = 0$. He found that for the region $0 \leqslant x \leqslant U_\infty t$ boundary conditions must be enforced at each 'end' of the region of interest (as $x \to 0$ the boundary-layer solution must approach the Blasius solution; as $x \to U_\infty t$ it must approach Rayleigh's solution). Later, Stewartson (1960) gave an interesting interpretation of this behaviour. It will be shown that in the present problem again two boundary conditions must be enforced for the boundary layer of the I region, in addition to the usual wall and free-stream conditions. Lam & Crocco (1958) discussed the more general problem of a shock advancing past a semi-infinite flat plate. (For the special case of weak shocks, the problem becomes identical with Stewartson's.) Using the boundary-layer equations in the Crocco form, they also found that in the general problem two boundary conditions must be enforced at $x = 0$ and $x = U_\infty t$, where U_∞ is the free-stream flow velocity of the fluid following the shock. They termed this region 'the interaction region', and the boundary-value problem 'singular-parabolic', following Gevrey (1914). It will be shown that the variables used by Lam & Crocco represent well the singular nature of the I region also in the present problem.

2. Formulation

We make the following assumptions: the two-dimensional laminar boundary-layer equations are valid; diffusion at the contact surface is negligible; the wall temperature, T_w, equals the initially uniform gas temperatures; the specific-heat ratios, k, and the Prandtl numbers, σ, are constant and equal for both gases. Also, U_s, c_l and U_0 are constant (see figure 1), as required by Riemann's solution; and so are the parameters

$$A = U_s/U_0, \quad B = c_l/U_0.$$

Crocco and others have used the dependent variables shear stress and specific enthalpy in boundary-layer problems:

$$\tau = \mu \frac{\partial u}{\partial y} = \tau(x, u, t), \quad h = h(x, u, t).$$

Here x is the distance along the wall, measured from the diaphragm location, u is the velocity component parallel to the wall, and t the time. In terms of these variables, the boundary-layer equations are

$$\frac{\partial^2 \tau}{\partial u^2} + \frac{\partial}{\partial t}\left(\frac{\rho\mu}{\tau}\right) = 0, \tag{2.1}$$

$$\rho\mu\left\{\frac{\partial h}{\partial t} + \frac{\partial h}{\partial x}\right\} + \frac{1}{2}\left(1 - \frac{1}{\sigma}\right)\frac{\partial}{\partial u}(\tau^2)\frac{\partial h}{\partial u} = \tau^2\left(1 + \frac{\partial}{\partial u}\left(\frac{hu}{\sigma}\right)\right).$$

The boundary conditions at the wall ($u = 0$, $h = h_w$), and at the free-stream boundary ($u = U_0$, $h = h_\infty$), lead to

$$\left(\tau\frac{\partial\tau}{\partial u}\right)_w = 0, \quad h(x,0,t) = h_w, \tag{2.2}$$
$$\tau(x,U_0,t) = 0, \quad h(x,U_0,t) = h_\infty.$$

The constant h_∞ (essentially the free-stream temperature) has different values $h_\infty^{(0)}$ and $h_\infty^{(1)}$ in the M region and in the I and L regions, respectively: $h_\infty^{(0)} > h_\infty^{(1)}$. The quantities U_0, U_s, h_0, h_1, A, B, are determined by the two parameters: initial pressure ratio, p_l/p_r, and wall temperature, T_w.

New dimensionless independent and dependent variables

$$\alpha = \frac{x}{U_0 t}, \quad \beta = \frac{u}{U_0}, \quad \gamma = \frac{\rho_w U_0^2 t}{\mu_w}, \tag{2.3}$$

$$\frac{\tau}{\rho_w U_0^2} = \frac{\phi(\alpha,\beta)}{\sqrt{\gamma}}, \quad H = \frac{h-h_w}{h_w} = H(\alpha,\beta) \quad \left(\text{i.e. } \frac{\partial H}{\partial\gamma} = 0\right), \tag{2.4}$$

are now introduced. Here we have anticipated the self-similar time-dependence common to shock-induced boundary-layer problems (see Rott 1964; Stewartson 1964, or Lam & Crocco 1958); for, on introducing (2.3) and (2.4) into (2.1), the governing equations become

$$\phi^2\frac{\partial^2\phi}{\partial\beta^2}+\frac{\phi}{2} = (\beta-\alpha)\frac{\partial\phi}{\partial\alpha}, \tag{2.5a}$$

$$\phi^2\left\{\frac{U_0^2}{h_w}+\frac{1}{\sigma}\frac{\partial^2 H}{\partial\beta^2}\right\}-\phi\frac{\partial\phi}{\partial\beta}\frac{\partial H}{\partial\beta}\left(1-\frac{1}{\sigma}\right) = (\beta-\alpha)\frac{\partial H}{\partial\alpha}, \tag{2.5b}$$

with boundary conditions

$$\frac{\partial\phi}{\partial\beta}(\alpha,0) = 0, \quad H(\alpha,0) = 0, \tag{2.6}$$

$$\phi(\alpha,1) = 0, \quad H(\alpha,1) = H_\infty = \begin{cases} \dfrac{h_\infty^{(0)}-h_w}{h_w} = H_0 & (M \text{ region}), \\[2ex] \dfrac{h_\infty^{(1)}-h_w}{h_w} = H_1 & (I \text{ and } L \text{ regions}). \end{cases}$$

This form of the equations, where (2.5a) is decoupled from (2.5b), presupposes validity of the viscosity law $\rho\mu = \rho_w\mu_w$ (Chapman–Rubesin).

The singular parabolic nature of the equations in the I region can now be seen. While in the M region, $1 \leqslant \alpha \leqslant A$, and in the L region, $0 \geqslant \alpha \geqslant -B$, the coefficient of the α-derivative in (2.5) has a constant sign, in the I region, $0 \leqslant \alpha \leqslant 1$, the coefficient of the α-derivative may take on both signs on $0 \leqslant \beta \leqslant 1$. In this region the boundary-layer equations permit two boundary conditions along the 'vertical' edges. This formulation is mathematically correct, at least for the linearized problems (3.7), (3.18), and was already foreseen as a mathematical possibility in Gevrey's (1914) treatise (see Ban 1967).

We now write out the specific forms of (2.8) in the three regions of interest and notice that in the M and L regions, the α- and β-dependences may be separated as follows.

$$M:\quad \phi(\alpha,\beta) = \left(\frac{A-1}{A-\alpha}\right)^{\frac{1}{2}} M(\beta), \quad H = H_M(\beta) \quad (1 \leqslant \alpha \leqslant A); \tag{2.7}$$

$$\begin{cases} MM'' + \dfrac{1}{2}\left(\dfrac{A-\beta}{A-1}\right) = 0, \quad M'(0) = M(1) = 0, & (2.8a) \\ M\left(\dfrac{U_0^2}{h_w} + \dfrac{1}{\sigma}H''_M\right) - M'H'_M\left(1-\dfrac{1}{\sigma}\right) = 0, \quad \begin{Bmatrix} H_M(0) = 0, \\ H_M(1) = H_0. \end{Bmatrix} & (2.8b) \end{cases}$$

$$L:\quad \phi(\alpha,\beta) = \left(\frac{B}{B+\alpha}\right)^{\frac{1}{2}} L(\beta), \quad H = H_L(\beta) \quad (-B \leqslant \alpha \leqslant 0); \tag{2.9}$$

$$\begin{cases} LL'' + \dfrac{1}{2}\left(1+\dfrac{\beta}{B}\right) = 0, \quad L'(0) = L(1) = 0, & (2.10a) \\ L\left(\dfrac{U_0^2}{h_w} + \dfrac{1}{\sigma}H''_L\right) - L'H'_L\left(1-\dfrac{1}{\sigma}\right) = 0. \quad \begin{Bmatrix} H_L(0) = 0, \\ H_L(1) = H_1. \end{Bmatrix} & (2.10b) \end{cases}$$

The forms (2.7) and (2.9) represent Mirels' similarity 'ansatz' in Crocco variables.

The problem in the I region ($0 \leqslant \alpha, \beta \leqslant 1$) can now be written out completely:

$$\begin{cases} \phi^2 \dfrac{\partial^2\phi}{\partial\beta^2} + \dfrac{\phi}{2} = (\beta-\alpha)\dfrac{\partial\phi}{\partial\alpha}, & (2.11a) \\ \phi^2 \left\{\dfrac{U_0^2}{h_w} + \dfrac{1}{\sigma}\dfrac{\partial^2 H}{\partial\beta^2}\right\} - \phi\dfrac{\partial\phi}{\partial\beta}\dfrac{\partial H}{\partial\beta}\left(1-\dfrac{1}{\sigma}\right) = (\beta-\alpha)\dfrac{\partial H}{\partial\alpha}, & (2.11b) \end{cases}$$

with boundary conditions

$$\frac{\partial\phi}{\partial\beta}(\alpha,0) = 0, \quad H(\alpha,0) = 0, \quad \phi(\alpha,1) = 0, \quad H(\alpha,1) = H_1, \tag{2.12a}$$

$$\left.\begin{aligned} \phi(0,\beta) = L(\beta), \quad \phi(1,\beta) = M(\beta), \\ H(0,\beta) = H_L(\beta), \quad H(1,\beta) = H_M(\beta). \end{aligned}\right\} \tag{2.12b}$$

The free-stream temperature jump across the contact discontinuity produces here a discontinuity (cf. (2.8)),

$$\lim_{\alpha\to 1} H(\alpha,1) = H_1 < \lim_{\beta\to 1} H(1,\beta) = H_0, \tag{2.13}$$

not unusual in heat-conduction problems.

We may compare this problem with that considered by Lam & Crocco (1958), which was described earlier. The two problems coincide in the M region where, as Lam & Crocco and Stewartson (1960) pointed out, the solution is independent of the I region. Also, Mirels solved the same problem in 1955. However, Lam & Crocco had no L region in their problem; instead, the shear stress had to approach Crocco's well known flat-plate solution as $\alpha \to 0$. In the present case the solutions in L and M must be known before the I region can be attacked. A further complication is the free-stream temperature jump across the contact discontinuity, which influences considerably the character of the solution for ϕ and H in the I region.

Seen from the viewpoint of modern analysis, uniqueness and existence of the solution to the linearized version of the present problem can be formulated by means of Friedrichs's (1958) theory (see appendix); and it has now received its proper place in the context of recent achievements in the theory of differential equations.

3. The linearized problem

3.1. *The momentum equation*

The parameters A and B in (2.7) and (2.8) determine the total length of the boundary layer at $t = t^*$ (see figure 2). From the definition of A and the well-known relation between shock speed and trailing gas velocity (see Courant & Friedrichs 1948, p. 151), we can write

$$A = \frac{U_s}{U_0} = \frac{k+1}{4}\left[\frac{kRT_w}{U_0^2} + \left(\frac{k+1}{4}\right)^2\right]^{\frac{1}{2}};$$

and, with the definition of $B \equiv c_l/U_0$, we have

$$A = \frac{k+1}{4} + \left[B^2 + \left(\frac{k+1}{4}\right)^2\right]^{\frac{1}{2}}, \tag{3.1}$$

from ideal shock-tube theory. From this we can note that the shock Mach number is given by

$$\frac{A}{B} = M_s = \frac{U_s}{c_l},$$

and $$M_s^2 \to 1 \Rightarrow B^2 \to A^2 \Rightarrow A^2 - \tfrac{1}{2}(k+1)\,A \to A^2,$$

so that $M_s^2 \gtrsim 1$ requires $A \gg 1$ (weak-wave condition), and $B \sim A$. Thus, the following expansions are proposed to produce a systematic linearization simultaneously in the three regions:

$$M = \sum_{i=0}^{\infty} \frac{M_i(\beta)}{A^i}, \quad L = \sum_{i=0}^{\infty} \frac{L_i(\beta)}{A^i}, \quad \phi = \sum_{i=0}^{\infty} \frac{\phi_i(\alpha,\beta)}{A^i},$$

with $$\frac{1}{B} = \frac{1}{A} + [\tfrac{1}{4}(k+1)]\frac{1}{A^2} + \dots,$$

used in (2.10). Substituting these expansions into the governing equations (2.8), (2.10), and (2.11) gives in the order $(1/A)^0$,

$$M_0(\beta) = L_0(\beta) = \phi_0(\beta).$$

Thus, to zeroth order, the shear stress is everywhere independent of α and satisfies the same two-point boundary-value problem

$$\phi_0\phi_0'' + \tfrac{1}{2} = 0, \quad \phi_0'(0) = \phi_0(1) = 0. \tag{3.2}$$

The solution to (3.2) is known. Denoting the inverse of the error function, $y = \mathrm{erf}^{-1}(x)$, by $\mathrm{fre}(x)$ $(-1 < x < 1)$, we have

$$\frac{dy}{dx} = \frac{\sqrt{\pi}}{2}e^{y^2}, \quad y(0) = 0, \tag{3.3}$$

as definition of fre (x). Thus,

$$\phi_0(\beta) = \frac{1}{\sqrt{\pi}} \exp[-\text{fre}^2(\beta)] \quad (= M_0 = L_0). \tag{3.4}$$

In the order of $(1/A)$ we get the first-order problem in the M and L regions:

$$M_1'' - \tfrac{1}{2}\pi \exp[2\,\text{fre}^2(\beta)]\, M_1 = (\beta - 1)\,\tfrac{1}{2}\sqrt{\pi} \exp[\text{fre}^2(\beta)],$$

$$M_1'(0) = 0, \quad M_1(1) = 0; \tag{3.5}$$

$$L_1'' - \tfrac{1}{2}\pi \exp[2\,\text{fre}^2(\beta)]\, L_1 = \tfrac{1}{2}\beta\sqrt{\pi} \exp[\text{fre}^2(\beta)],$$

$$L_1'(0) = 0, \quad L_1(1) = 0. \tag{3.6}$$

The two functions L_1 and M_1 yield the first-order boundary conditions on the function $\phi_1(\alpha, \beta)$ in the I region. Equations (3.5) and (3.6) are again two-point boundary-value problems, but $\beta = 1$ is now a singular point of the equations, since fre $(1) = \infty$. Its solution, together with the determination of fre (β) and $\phi_0(\beta)$, will be discussed in a later section.

The first-order problem for ϕ_1 in the I region can now be set up:

$$\phi_0^2 \frac{\partial^2 \phi_1}{\partial \beta^2} - \frac{\phi_1}{2} = (\beta - \alpha) \frac{\partial \phi_1}{\partial \alpha}; \tag{3.7a}$$

$$\left.\begin{aligned} &\frac{\partial \phi_1}{\partial \beta}(\alpha, 0) = 0, \quad \phi_1(\alpha, 1) = 0, \\ &\phi_1(0, \beta) = L_1(\beta), \quad \phi(1, \beta) = M_1(\beta). \end{aligned}\right\} \tag{3.7b}$$

Equation (3.7a) is a linear, singular parabolic equation. Thus the boundary conditions can be prescribed on all four sides of the quadratic I region. Once ϕ_0, L_1 and M_1 are known, the solution of problem (3.7) should be possible.

3.2. *The energy equation*

The governing energy equations are treated in the same manner. We write again

$$H_M = \sum_{i=0}^{\infty} \frac{H_{M_i}(\beta)}{A^i}, \quad H_L = \sum_{i=0}^{\infty} \frac{H_{L_i}(\beta)}{A^i}, \quad H(\alpha, \beta) = \sum_{i=0}^{\infty} \frac{g_i(\alpha, \beta)}{A^i},$$

and also expand $H_0 - H_1$ in terms of $(1/A)$ as

$$H_0 = H_1 + \frac{2(k-1)}{A} + \ldots,$$

for the boundary condition in (2.8b). The constant U_0^2/h_w in the energy equations, which depends on the data p_r/p_l and T_w and arises from viscous dissipation, must be replaced according to

$$\frac{U_0^2}{h_w} = \frac{(k-1)\,M_s^2}{A^2} = \frac{k-1}{A^2 - \frac{1}{2}(k+1)A} = \frac{k-1}{A^2}\left[1 + \frac{k+1}{2A} + \left(\frac{k+1}{2A}\right)^2 + \ldots\right].$$

Substituting and ordering in $(1/A)$ gives in zeroth order

$$H_{L_0} = H_{M_0} = g_0(\beta),$$

where $g_0(\beta)$ is to be determined from

$$\left.\begin{aligned}\frac{\phi_0}{\sigma}g_0''-\phi_0'g_0'\left(1-\frac{1}{\sigma}\right)&=0,\\ g_0(0)=0,\quad g_0(1)&=H_1.\end{aligned}\right\}\tag{3.8}$$

With ϕ_0 known from (3.4),

$$g_0=H_1[\operatorname{erf}(\sqrt{\sigma}\operatorname{fre}(\beta)].\tag{3.9}$$

As before, the first-order problems can now be written in the M and L regions:

$$\frac{\phi_0}{\sigma}H_{M_1}-\left(1-\frac{1}{\sigma}\right)\phi_0'H_{M_1}'=\left(1-\frac{1}{\sigma}\right)M_1'g_0'-M_1\frac{g_0''}{\sigma},$$

$$H_{M_1}(0)=0,\quad H_{M_1}(1)=2(k-1);\tag{3.10}$$

$$\frac{\phi_0}{\sigma}H_{L_1}''-\left(1-\frac{1}{\sigma}\right)\phi_0'H_{L_1}'=\left(1-\frac{1}{\sigma}\right)L_1'g_0'-L_1\frac{g_0''}{\sigma},\quad H_{L_1}(0)=0,\quad H_{L_1}(1)=0.\tag{3.11}$$

The first-order problem in the I region is

$$\frac{\phi_0^2}{\sigma}\frac{\partial^2g_1}{\partial\beta^2}-\left(1-\frac{1}{\sigma}\right)\phi_0\phi_0'\frac{\partial g_1}{\partial\beta}-(\beta-\alpha)\frac{\partial g_1}{\partial\alpha}=\left(1-\frac{1}{\sigma}\right)\left(\phi_0'g_0'\phi_1+\phi_0g_0'\frac{\partial\phi_1}{\partial\beta}\right)-2\phi_0\phi_1\frac{g_0''}{\sigma};\tag{3.12a}$$

$$g_1(\alpha,0)=0,\quad g_1(\alpha,1)=0,\quad g_1(0,\beta)=H_{L_1}(\beta),\quad g_1(1,\beta)=H_{M_1}(\beta).\tag{3.12b}$$

This again is a singular parabolic equation. The function $g_1(\alpha,\beta)$ can be determined once H_{L_1} and H_{M_1} have been found from (3.10) and (3.11).

For the purpose of a numerical example built on the zeroth and first approximations only, and in the interest of simplifying equation (3.12a) without changing its singular character, we take the Prandtl number, σ, equal to one. With this, the zeroth energy equation (3.8) becomes

$$\phi_0g_0''=0,\quad g_0(0)=0,\quad g_0(1)=H_1,\tag{3.13}$$

with solution

$$g_0=H_1\beta.\tag{3.14}$$

The corresponding first-order problems are

$$\phi_0H_{M_1}''=-M_1g_0''=0;\quad H_{M_1}(0)=0,\quad H_{M_1}(1)=2(k-1),\tag{3.15}$$

$$\phi_0H_{L_1}''=0;\quad H_{L_1}(0)=0,\quad H_{L_1}(1)=0.\tag{3.16}$$

The solutions to (3.15) and (3.16) are seen to be

$$H_{M_1}=2(k-1)\beta;\quad H_{L_1}=0.\tag{3.17}$$

The simplified first-order energy equation in the I region with completely defined boundary conditions can now be written down:

$$\phi_0^2\frac{\partial^2g_1}{\partial\beta^2}=(\beta-\alpha)\frac{\partial g_1}{\partial\alpha};\tag{3.18a}$$

$$g_1(\alpha,0)=0,\quad g_1(\alpha,1)=0,\quad g_1(0,\beta)=0,\quad g_1(1,\beta)=2(k-1)\beta.\tag{3.18b}$$

Note that the free-stream temperature jump across the contact discontinuity (cf. (2.13)) is still in the boundary conditions (3.18b).

4. Numerical solution

We first take up the numerical determination of fre(β) defined by (3.3). The Runge–Kutta–Gill method was used to integrate this equation numerically instead of inverting the error function. Once fre(β) is known the zeroth-order shear stress given by (3.4) can be computed pointwise. The functions fre(β) and $\phi_0(\beta)$ are shown in figure 3.

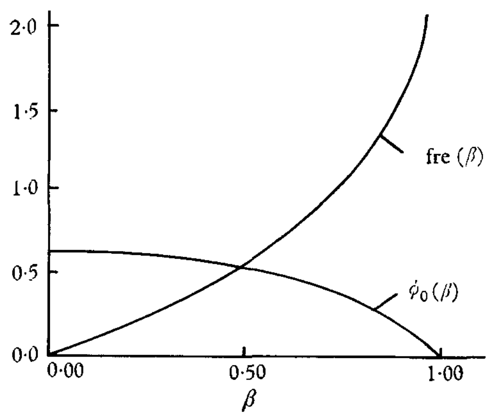

FIGURE 3. The functions fre(β) and $\phi_0(\beta)$.

The functions $M_1(\beta)$ and $L_1(\beta)$ give the β variation of the first-order shear stress in L and M. It is to be noticed that both equations (3.5) and (3.6) have essential singularities at $\beta = 1$, making the numerical solution difficult. Although not designed for singular problems, the method of factorization of Ridley (1957) was found to be successful. Ridley replaces the second-order equation by three first-order equations that automatically satisfy the two-point boundary conditions if the starting values $(L_1(0), M_1(0))$ can be guessed. Initial approximations to these starting values were obtained from approximate predictor–corrector solutions to these equations. The initial approximations were then adjusted until the boundary condition at $\beta = 1$ was satisfied to six decimal places. The functions $M_1(\beta)$ and $L_1(\beta)$ obtained in this manner are shown in figure 4.

The determination of the first-order functions in the I region requires the solution of the singular parabolic differential equations (3.7) and (3.18) and is considerably more difficult. Standard 'forward marching' parabolic techniques cannot be used. Instead, numerical methods normally used in elliptic problems must be applied. The technique used will be outlined here; the details can be found in Ban (1967).

If one replaces (3.7a) and (3.18a) by a set of difference equations, following e.g. Forsythe & Wasow (1960), one notices that an important condition is not satisfied: due to the parabolic form of (3.7) and (3.18), the coefficient matrix of the set is not diagonally dominant. Because of this, all standard *explicit* iterative techniques (those in which the kth approximation to the unknown at a point can be determined from knowledge at hand explicitly) that depend heavily on diagonal dominance for convergence (simultaneous displacements, Gauss–Seidel, successive over-relaxation, etc.) will not succeed.

There are, however, *implicit* techniques in which, within the set of the unknown function values at the mesh points, blocks of unknowns are defined by the iteration, so that the kth approximation to any member of the block is known implicitly after all members of the block have been determined simultaneously.

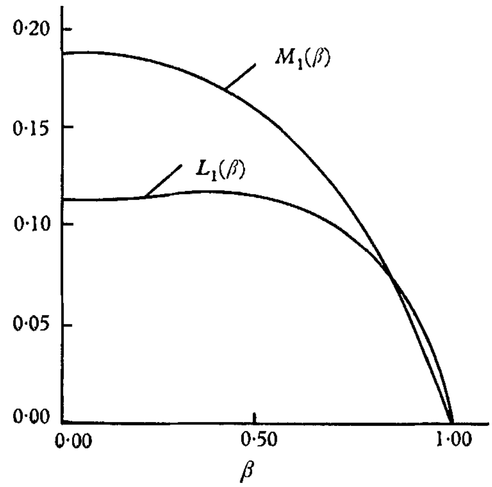

FIGURE 4. The first-order boundary conditions.

ζ	$\phi_0(\zeta)$	$M_1(\zeta)$	$L_1(\zeta)$	$\phi_1(\zeta,0)$	$\eta_\delta(\zeta)$
0	0·56419	0·17960	0·10240	0·10240	3·457
0·1	0·55075	0·17672	0·10306	0·07364	3·475
0·2	0·54637	0·16861	0·10447	0·04583	3·492
0·3	0·52382	0·15601	0·10580	0·02617	3·510
0·4	0·49171	0·13956	0·10619	0·02667	3·523
0·5	0·33940	0·11989	0·10469	0·04342	3·531
0·6	0·39593	0·09763	0·10020	0·06759	3·535
0·7	0·32974	0·07345	0·09127	0·09512	3·538
0·8	0·24819	0·04811	0·07581	0·12315	3·543
0·9	0·14586	0·02273	0·04999	0·15118	3·560
1·0	0·00000	0·00000	0·00000	0·17960	3·691

TABLE 1. Summary of numerical results

The implicit technique of *successive displacements by lines* (see Forsythe & Wasow 1960) was found to be rapidly convergent in the case of both the momentum and energy equations. In this method, the successive-displacement iteration takes place between blocks of unknowns (in our case, lines of constant β) while within each block the function values are solved for simultaneously from a linear subsystem relating the members of that block. This method is not so heavily dependent on the character of the coefficient matrix alone, but rather on the way in which the unknowns are broken up into blocks. The convergence rate, although adequate, was improved markedly by using a direct solution obtained by Gauss elimination for a very coarse mesh (100 points, step size 0·1) as the initial guess to start the iteration. The functions $\phi_1(\alpha, \beta)$ and $g_1(\alpha, \beta)$ (for $k = 1{\cdot}4$) obtained in this manner are given in figures 5 and 6. A summary of numerical results is contained in table 1.

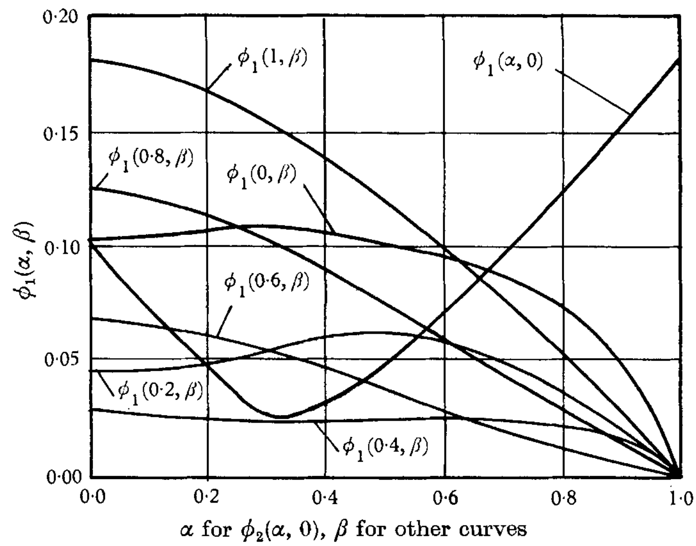

FIGURE 5. The first-order shear stress in the I region, $\phi_1(\alpha, \beta)$.

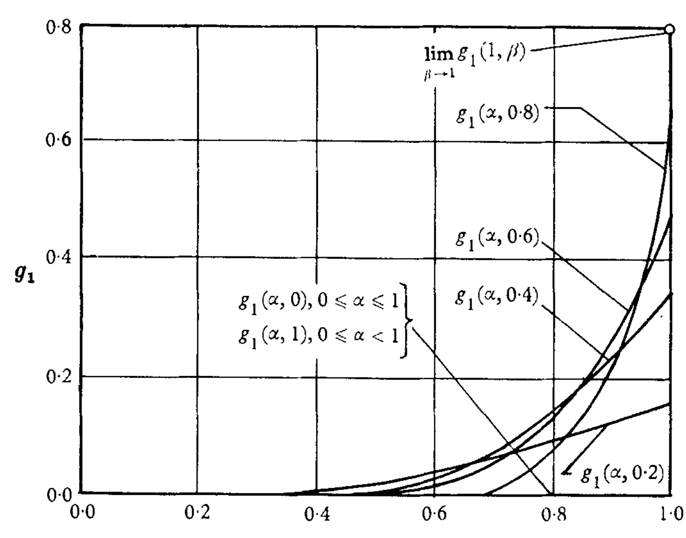

FIGURE 6. The first-order enthalpy function in the I region, $g_1(\alpha, \beta)$ ($\sigma = 1$, $k = 1{\cdot}4$).

5. Results

With the solution for the first-order functions completed, we can now examine the resulting behaviour of the solution in terms of the physical variables of interest for a particular set of parameter values. We examine the flow resulting from the initial conditions

$$p_l/p_r = 1{\cdot}35, \quad T_w = 293{\cdot}2K, \quad p_l = 1\,\text{atm}.$$

From these, together with the inviscid shock-tube relations and the perfect-gas state-equation, the following quantities are found:

$$p_0/p_r = 1{\cdot}16, \quad U_0 = 120{\cdot}9\,\text{ft./s}, \quad U_s = 1202{\cdot}9\,\text{ft./s},$$
$$A = 9{\cdot}95, \quad B = 9{\cdot}33, \quad M_s = 1{\cdot}06, \quad H_1 = -0{\cdot}0422,$$

for an air–air shock tube ($k = 1{\cdot}4$).

We first show the variation of the wall shear stress for the complete shock tube ($-B \leqslant \alpha \leqslant A$) for this case. By writing (from (2.7) and (2.4))

$$\tau_w = \left(\mu\frac{\partial u}{\partial y}\right)_w = \rho_w U_0^2 \frac{\phi(\alpha, 0)}{\sqrt{\gamma}} = \left(\frac{\rho_w U_0^2 \mu_w}{t}\right)^{\frac{1}{2}} \phi(\alpha, 0),$$

we have to first order

$$\phi(\alpha, 0) \sim \phi^{(1)}(\alpha, 0) = \left\{\begin{array}{ll} \left(\phi_0(0) + \dfrac{L_1(0)}{A}\right)\left(\dfrac{B}{B+\alpha}\right)^{\frac{1}{2}} & (-B \leqslant \alpha \leqslant 0), \\ \phi_0(0) + \dfrac{\phi_1(\alpha, 0)}{A} & (0 \leqslant \alpha \leqslant 1), \\ \left(\phi_0(0) + \dfrac{M_1(0)}{A}\right)\left(\dfrac{A-1}{A-\alpha}\right)^{\frac{1}{2}} & (1 \leqslant \alpha \leqslant A), \end{array}\right\} \tag{5.1}$$

$$\frac{\tau_w}{\rho_w U_0^2}\left(\frac{\rho_w U_0^2 t}{\mu_w}\right)^{\frac{1}{2}} \sim \phi^{(1)}(\alpha, 0).$$

This dimensionless wall shear is shown in figure 7.

We now take up the inversion of the velocity to the actual physical (x, y)-plane. From the definition of the transformed variables,

$$\frac{\partial u}{\partial y} = \left(\frac{\rho_w U_0^2 \mu_w}{t}\right)^{\frac{1}{2}} \frac{\phi(\alpha, \beta)}{\mu(\alpha, \beta)};$$

so that

$$y\left(\alpha, \frac{u}{U_0}\right) = U_0 \int_0^\beta \left(\frac{t}{\rho_w U_0^2 \mu_w}\right)^{\frac{1}{2}} \frac{\mu(\alpha, \xi)}{\phi(\alpha, \xi)} d\xi.$$

and, for a perfect gas (R = gas constant)

$$\mu = \frac{\rho_w \mu_w}{\rho} = \frac{\rho_w \mu_w R h}{c_p p_0} = \frac{\rho_w \mu_w}{p_0}\left(\frac{k-1}{k}\right)(h_w H + h_w),$$

on approximating ϕ by $\phi^{(1)}$ and H by $H^{(1)}$, we have for the dimensionless ordinate

$$\eta\left(\alpha, \frac{u}{U_0}\right) = \frac{y}{\left[\dfrac{(\rho_w \mu_w t)^{\frac{1}{2}} h_w}{p_0\left(\dfrac{k}{k-1}\right)}\right]} = \int_0^\beta \frac{H^{(1)}(\alpha, \xi) + 1}{\phi^{(1)}(\alpha, \xi)} d\xi. \tag{5.2}$$

Here $\phi^{(1)}(\alpha,\beta)$ is given by (5.1) and $H^{(1)}(\alpha,\beta)$ is given by (5.3)

$$H^{(1)}(\alpha,\beta) = \begin{cases} H_1\beta & (-B \leqslant \alpha \leqslant 0), \\ H_1\beta + \dfrac{g_1(\alpha,\beta)}{A} & (0 \leqslant \alpha \leqslant 1), \\ H_1\beta + \dfrac{2(k-1)\beta}{A} & (1 < \alpha \leqslant A). \end{cases} \tag{5.3}$$

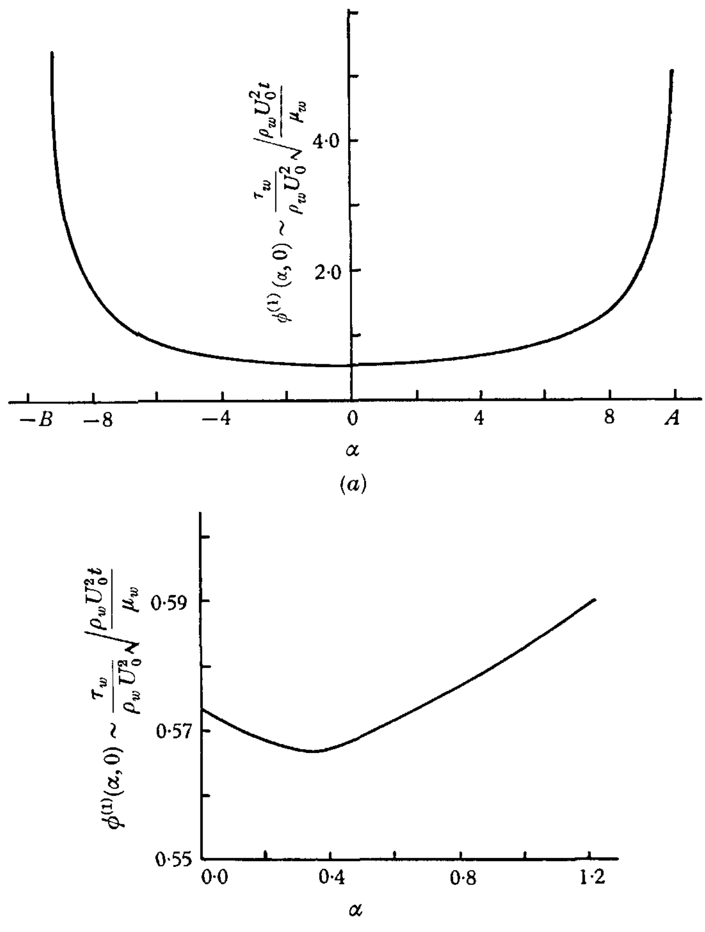

FIGURE 7. Wall shear stress (*a*) throughout entire flow field, (*b*) in *I* region.

In evaluating the dimensionless ordinate $\eta(\alpha, u/U_0)$, the integral appearing in (5.2) was evaluated at fixed α for various β-values, essentially by a Simpson-rule procedure. This gives profiles at various α of $\eta(\alpha, u/U_0)$, which may be regarded as velocity profiles $(u/U_0)(\eta)$ at various locations α in the shock tube (figure 8). The profile near the expansion was evaluated at $\alpha = (-0{\cdot}99B)$ and near the shock at $\alpha = (0{\cdot}99A)$. The results show that the boundary layer is quite thin near A and $-B$ and thickens away from them. The general profiles are all smooth and validate the assumption implicit in the Crocco transformation that $u(x, y, t)$ is a monotonically increasing function of y through the boundary layer. The correct velocity profiles in the L and M regions should be self-similar according to Mirels' (1956) results (see remark after (2.10*b*)), but the present profiles, being only approximations of first order, are not strictly self-similar.

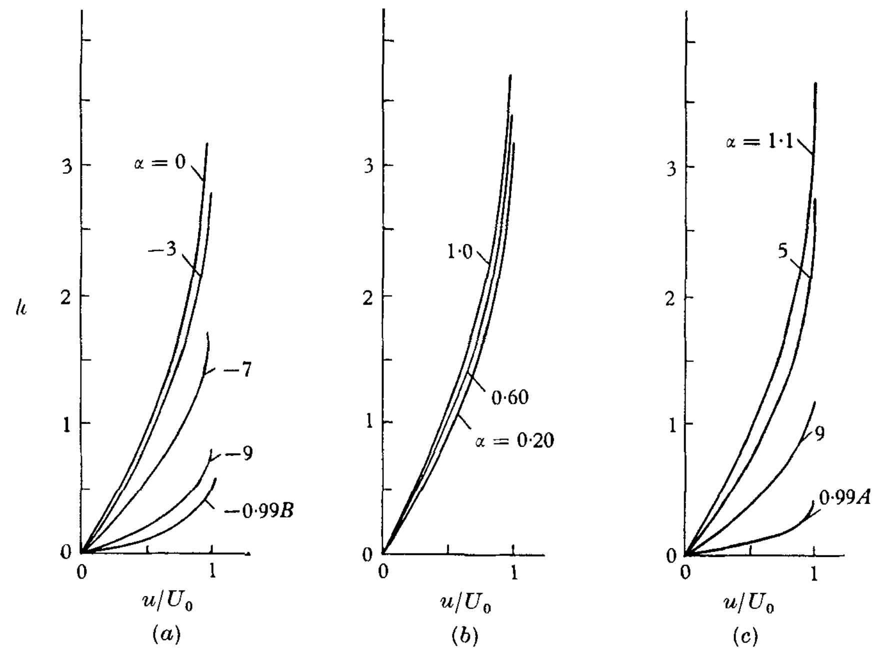

FIGURE 8. Velocity profiles (*a*) in L region, (*b*) in I region, (*c*) in M region.

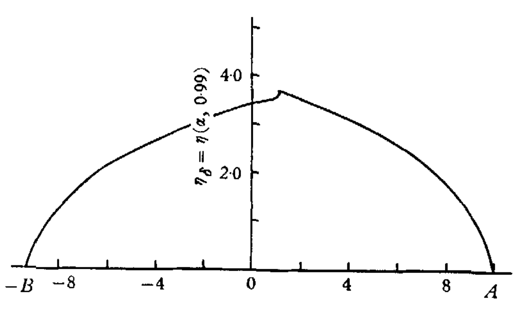

FIGURE 9. Variation of boundary-layer thickness.

We can now examine the variation in boundary-layer thickness over the length of the tube. Taking the boundary-layer edge to be at $\beta = 0{\cdot}99$, we can determine the variation of $\eta(\alpha, 0{\cdot}99) \equiv \eta_\delta$ (figure 9 and table 1).

We note the interesting fact that, near the contact discontinuity ($0{\cdot}9 < \alpha < 1$), there is a rapid but continuous (see figure 11) thickening of the boundary layer with the maximum boundary-layer thickness occurring at $\alpha = 1{\cdot}0$. Since $\phi_1(\alpha, \beta)$ does not vary rapidly with α in this region, the behaviour of the result of the integration (5.2) is caused mainly by the temperature jump in the boundary condition. From (5.1) and (5.2) we have

$$\eta_\delta \sim \int_0^{0\cdot 99} \frac{H_1\zeta+1}{\phi_0(\zeta)}\,d\zeta + \frac{1}{A}\int_0^{0\cdot 99} \frac{g_1(\alpha,\zeta)}{\phi_0(\zeta)}\,d\zeta,$$

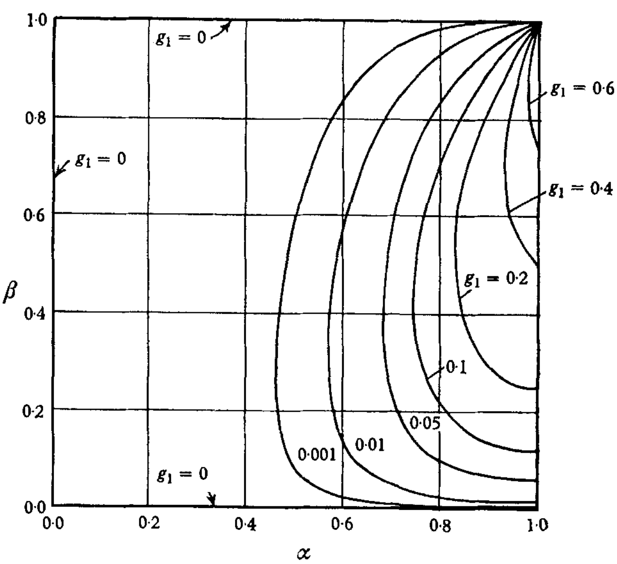

FIGURE 10. First-order isotherms as obtained from the numerical solution for $g_1(\alpha, \beta)$.

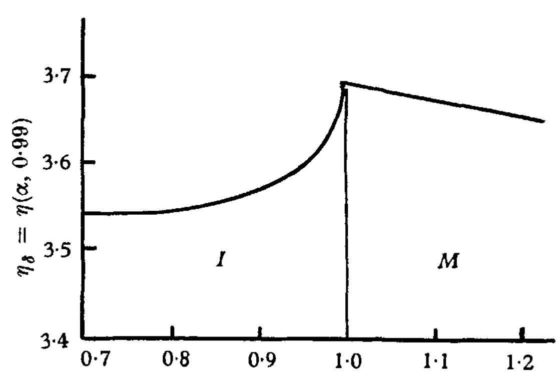

FIGURE 11. Boundary-layer thickness near $\alpha = 1$.

where we retain only terms up to first order in $1/A$. This leads to

$$\frac{d\eta_\delta}{d\alpha} \sim \frac{1}{A}\int_0^{0\cdot 99} \frac{1}{\phi_0(\zeta)}\frac{\partial}{\partial\alpha}g_1(\alpha,\zeta)\,d\zeta. \tag{5.4}$$

From figure 6, the slopes $\partial g/\partial\alpha$ are seen to practically vanish for $0 \leqslant \alpha \leqslant 0\cdot 4$. Here η_δ must be nearly constant. If we now compare contributions of the same $d\zeta$ to the integral in (5.4) for α_1, α_2, with $\alpha_1 < \alpha_2$, then from figure 6 it is seen that the second contribution is always greater than the first. This implies that $d\eta_\delta/d\alpha$ increases with α and the η_δ curve is concave upward, at least from some α-value on, up to $\alpha = 1\cdot 0$. Thus, the rapid steepening of the η_δ curve is a direct consequence of the singularity of the thermal boundary conditions at the point $\alpha = \beta = 1{\cdot}0$ (i.e. the location of the temperature jump), where the slopes $(\partial/\partial\alpha)[g_1(\alpha, \beta)]$ become large and dominate expression for $\partial\eta_\delta/\partial\alpha$. The same result could be read off figure 10, which shows the crowding of the first-order isotherms in the neighbourhood of $\alpha = \beta = 1$. This phenomenon is typical for certain parabolic problems with a jump discontinuity in the boundary values. Figure 11 illustrates the growth of $\eta_\delta(\alpha)$ by a large-scale diagram of the numerical results (table 1) near $\alpha = 1$.

6. Conclusion

The problem of the shock-tube boundary layer has been treated by a systematic linearization scheme that shows directly the singular parabolic nature of the governing equations. An important result is the applicability of the 'Crocco variables' to the numerical solution of the shock-tube problem despite the crowding at the boundary-layer edge, $\beta = 1$. The solution of the governing equations has been carried out in all three regions of the problem in this same set of variables, which is particularly advantageous, because the equations then evidence explicitly the analytic character of the problem.

The numerical results obtained for the example problem indicate that, physically, the effect of the contact discontinuity is small, at least for the case of weak shocks. The only apparent effect is a layer thickening that is less than 5 % of the total thickness near the M–I boundary with a continuous transition of the thickness parameter from L to I to M. This, as well as the zero-order α-independent solution, shows further that (to first order) there are no boundary-layer eruptions in the interaction region and that any such behaviour must enter as a higher-order effect.

The work also demonstrates that the numerical solution of a singular parabolic equation is possible when a particular numerical method devised for elliptic equations is used. We know of no example in numerical analysis for this type of partial differential equation.

The retransformation of the solution from the Crocco plane to the physical plane gave velocity profiles throughout the whole boundary layer, including the behaviour near the contact discontinuity.

Finally, the place of the linearized problem within current theory of differential equations is pointed out in the appendix.

From the standpoint of usefulness, the major limitations of the study are: consideration of a shock tube with the same driver and driven gas; limitation to weak expansion waves. This latter restriction was introduced mainly to permit concentration of the numerical effort on the linear problem in the I region.

The authors wish to acknowledge several helpful suggestions given by Dr K. Stewartson. They would also like to thank Dr E. Reshotko for many valuable discussions during the later stages of the analysis. This research was supported in part by the National Science Foundation and the Air Force Office of Scientific Research.

Appendix

For a thorough discussion of the existence theory of (3.7) in terms of Friedrichs (1958) and Gevrey (1914), we must refer the reader to Ban (1967). Here only those results that follow readily from Friedrichs's study for our case will be presented.

Problem (3.7) for $\phi_1(\alpha,\beta)$ can be made to fit into Friedrichs's algebraic scheme, when the homogeneous second-order equation (3.7*a*) with inhomogeneous boundary conditions (3.7*b*) is replaced by the inhomogeneous first-order pair (in matrix notation)

$$\left\{\begin{pmatrix} 0 & -1 \\ -1 & 0 \end{pmatrix}\frac{\partial}{\partial\beta}+\begin{pmatrix} 2(\alpha-\beta)P & 0 \\ 0 & 0 \end{pmatrix}\frac{\partial}{\partial\alpha}+\begin{pmatrix} P & 0 \\ 0 & 1 \end{pmatrix}\right\}\begin{bmatrix} u_1 \\ u_2 \end{bmatrix}=\begin{bmatrix} 2hP \\ 0 \end{bmatrix}. \tag{A 1}$$

Here $P(\beta)=\frac{1}{2}[\phi_0(\beta)]^{-2}$ is positive for $0\leqslant\beta<1$ and not bounded; $u_1\equiv -U$, $u_2\equiv -U_\beta$; $U\equiv\phi_1(\alpha,\beta)-F(\alpha,\beta)$; $z=F(\alpha,\beta)$ is the ruled surface generated by sliding a straight edge, which is parallel to the (α,z)-plane, along the boundary curves $z=L_1(\beta)$ above $\alpha=0$ and $z=M_1(\beta)$ above $\alpha=1$; and

$$-h(\alpha,\beta)\equiv\phi_0^2F_{\beta\beta}-(\beta-\alpha)F_\alpha-\tfrac{1}{2}F.$$

According to Friedrichs's theory, *admissible* boundary conditions for the rectangular domain $0\leqslant\alpha\leqslant 1$, $0\leqslant\beta\leqslant 1-\epsilon$, $\epsilon>0$ are

$$U(0,\beta)=U(1,\beta)=U(\alpha,1-\epsilon)=U_\beta(\alpha,0)=0. \tag{A 2}$$

Admissible boundary conditions imply existence of a weak solution and uniqueness of a 'classical' solution if it exists. The actual (physical) boundary conditions for ϕ_1, (3.7*b*), are obtained if we put $\epsilon=0$. However, whether this is a permissible step is not obvious and requires a mathematical investigation beyond the scope of this work.

REFERENCES

Ban, S. 1967 *Case-Institute Rept.* FTAS/TR-67-20, AFOSR *Sci. Rept.* 67-1286.

Becker, E. 1962 *Z. Flugwiss.* **10**, 4/5, 138.

Cohen, N. 1957 NACA TN 3943.

Courant, R. & Friedrichs, K. 1948 *Supersonic Flow and Shock Waves.* New York: Interscience.

Friedrichs, K. 1958 *Comm. Pure Appl. Math.* **11**, 333.

Forsythe, G. & Wasow, W. 1960 *Finite Difference Methods for Partial Differential Equations.* New York: Wiley.

Gevrey, M. 1914 *J. Math.* **10** (6).

Lam, H. & Crocco, L. 1958 *Princeton Rept.* 428, AFOSR TN 58-581.

Mirels, H. 1955 NACA TN 3401.

Mirels, H. 1956 NACA TN 3712.

Ridley, E. 1957 *Proc. Camb. Phil. Soc.* **53**, 442.

Rott, N. 1964 Theory of Laminar Flows. *High Speed Aero. and Jet Propulsion* **4** (F. K. Moore, ed.). Princeton University Press.

Stewartson, K. 1951 *Quart. Appl. Math. Mech.* **4**, 182.

Stewartson, K. 1960 *Adv. Appl. Mech.* **6**, 1.

Stewartson, K. 1964 *The Theory of Laminar Boundary Layers in Compressible Fluids.* Oxford University Press.